FRONTIERS OF PHYSICS

RESEARCH ARTICLE
Volume 19 / Issue 3 / 32202 / 2024

Phonon-blockade-based multiple-photon bundle emission in a quadratically coupled optomechanical system

Ye-Jun Xu[1,†], Hong Xie[2,‡]

1 Interdisciplinary Research Center of Quantum and Photoelectric Information, Chizhou University, Chizhou 247000, China
2 Department of Mathematics and Physics, Fujian Jiangxia University, Fuzhou 350108, China
E-mail: †yejunxu@126.com, ‡xh@fjjxu.edu.cn
Received July 18, 2023; accepted September 26, 2023

ABSTRACT

We propose a scheme to realize antibunched multiple-photon bundles based on phonon blockade in a quadratically coupled optomechanical system. Through adjusting the detunings to match the conditions of phonon blockade in the photon sidebands, we establish super-Rabi oscillation between zero-photon state and multiple-photon states with adjustable super-Rabi frequencies under appropriate single-phonon resonant conditions. Taking the system dissipation into account, we numerically calculate the standard and generalized second-order functions of the cavity mode as well as the quantum trajectories of the state populations with Monte Carlo simulation to confirm that the emitted photons form antibunched multiple-photon bundles. Interestingly, the desirable n-photon states are reconstructed after a direct phonon emission based on phonon blockade, and thus the single-phonon emission heralds the cascade emission of n-photon bundles. Our proposal shows that the optomechanical system can simultaneously behave as antibunched multiple-photon emitter and single-phonon gun. Such a nonclassical source could have potential applications in quantum information science.

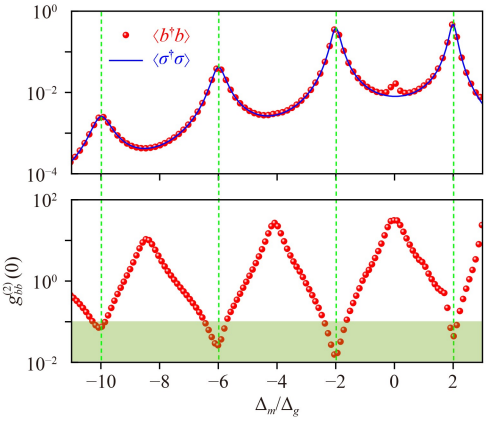

Keywords multiple-photon bundle emission, phonon blockade, optomechanical system

1 Introduction

Preparation of nonclassical quantum states has always been an interesting and significant research topic in quantum physics. The significance of this subject not only is very useful for studying fundamental quantum physics [1–3], but also has potential applications in quantum information science [4–12]. So far, much effort has been devoted to the generation of multiple-quanta states in various physical systems such as cavity quantum electrodynamics (QED) systems [13–19], waveguide QED systems [20–22], circuit QED systems [23], multiple-level atomic systems [24–28], Rydberg atomic ensembles [29, 30], cavity optomechanical systems [31], and hybrid magnet-qubit systems [32]. One of the interesting aspects of these previous works is that n-quanta bundle states can be generated by emitting multiple-quanta bundles with the energy unit of a bundle of several quanta [13–19, 23, 31, 32], and thus provide a mechanism for the realization of controllable multiple-quanta sources. In particular, Lü and co-workers pointed out that the single-photon emission event can act as the omen of the cascade emission of n-phonon bundles [15], since the system reconstructs the n-phonon state accom-

Higher Education Press

https://doi.org/10.1007/s11467-023-1352-9

panied by a photon emission arising from the quantum dot flip. However, cascade emission of n-photon bundles through releasing direct single phonon between both neighboring bundles is still an interesting but open issue.

Cavity optomechanics [33–37], exploring the nonlinear interaction via radiation-pressure force, has achieved great advances in both experimental and theoretical aspects for the past few decades. Among recent theoretical works, studies of optomechanical systems at the few-quantum level play an indispensable role and have predicted many interesting nonlinear quantum effects [38–44], even though it has remained a challenge to observe single-photon optomechanical effects with current experimental techniques. For example, phonon blockade is a kind of typical quantum phenomenon at the few-quantum level [45–50]. In analogy to photon blockade [51–62] and magnon blockade [63–67], phonon blockade is induced by mechanical anharmonicity ladder of energy spectrum with strong nonlinear interaction or destructive interference between different excitation paths. Phonon blockade provides a promising way to realize single-phonon source in which the presence of one phonon inhibits the excitation of the second phonon in a nonlinear mechanical oscillator. In addition, we notice that optomechanical system had been applied to investigate dynamical emission of phonon pairs based on the technique of stimulated Raman adiabatic passage [31]. One question that arises naturally is whether n-photon bundle emission can be realized in optomechanical system, even without using the technique of stimulated Raman adiabatic passage.

Motivated by previous proposals, here we propose a method to explore the antibunched n-photon bundle emission based on phonon blockade in a optomechanical system with quadratic coupling. The photon-assisted single-phonon transitions are achieved by the strong nonlinear photon-phonon interactions, in which the effective nonlinear coupling strength can be tuned by adjusting the amplitude of the driving field. Especially, the phonon blockade in the photon sidebands leads to the mechanical mode being in the zero-phonon state or the single-phonon state. As a result, the super-Rabi oscillation between the zero-photon state and the n-photon state can occur under the phonon blockade. Different from the previous work [15], here the n-photon emission is accompanied by emitting a single-phonon by reason of the phonon blockade effect and the system dissipation. Additionally, Ref. [31] depends on the technique of stimulated Raman adiabatic passage to realize an antibunched phonon-pair gun, here our approach has a different physical mechanism for achieving super-Rabi oscillations, i.e., through the photon-assisted single-phonon transitions. Consequently, the controllable characteristic of the phonon blockade in the photon sidebands can switch on/off the occurrence of the n-photon bundle emission. Our work associates the preparation of n-photon bundle state with the single-phonon state generated by the phonon blockade and offers a feasible strategy for simultaneously realizing antibunched multiple-photon cascade emission and antibunched single-phonon emission in the optomechanical system.

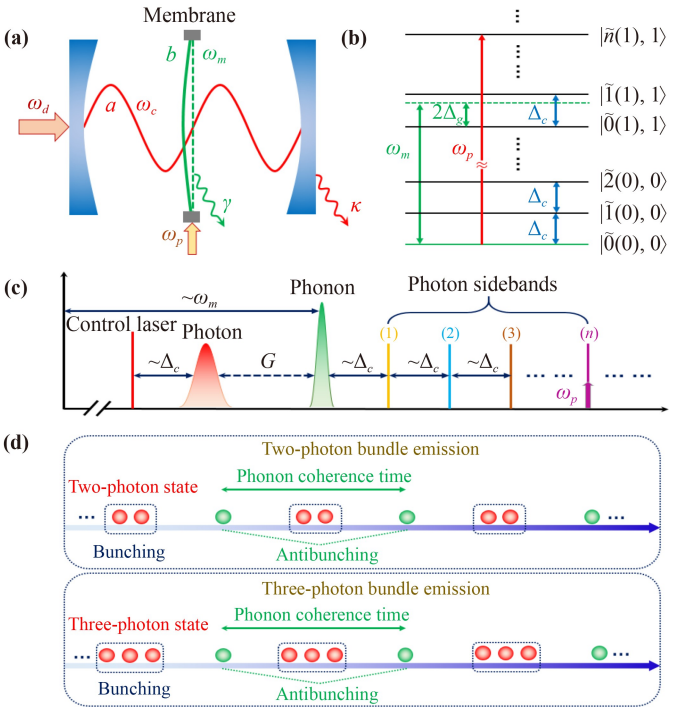

Fig. 1 **(a)** Schematic diagram of a quadratically coupled optomechanical system with a "membrane-in-middle" configuration. **(b)** Anharmonic energy-level diagram limited in the subspace spanned by the zero- and one-phonon states. States labelled as $|\tilde{n}(m), m\rangle$ denote the cavity mode being in m-phonon-dependent displaced Fock state and the mechanical mode being in m-phonon state. **(c)** Frequency spectrogram of the driven optomechanical system with quadratic coupling. There are high-order sidebands due to the nonlinear optomechanical interaction. **(d)** Illustration of cascade emission of antibunched n-photon ($n = 2, 3$) bundles, where the system releases each photon bundle accompanied by single-phonon emission.

The remainder of this paper is organized as follows. In Section 2, we describe the theoretical model of a strongly driven optomechanical system with quadratic coupling and derive the approximate effective Hamiltonian under the single-phonon resonances. In Section 3, we study the eigensystem of the system in the displaced representation and establish the super-Pabi oscillation between the zero-photon state and the n-photon ($n = 2, 3$) state under proper resonant condition. We discuss the statistical properties of the multiple-photon bundle emission by numerically calculating the standard equal time high-order correlation functions, the standard and generalized time-delay second-order correlation functions, and the Monte Carlo simulations of state populations in Section 4. Finally, we give some discussions

on the experimental realization and the main results are summarized in Section 5.

2 Model and Hamiltonian

As shown in Fig. 1(a), we consider a quadratically coupled optomechanical system with a membrane-in-the-middle configuration, in which a thin dielectric membrane is located in a node (or antinode) of the intracavity standing wave inside a Fabry–Pérot cavity. In addition, we assume that a strong laser field with frequency ω_{d} is applied to drive the cavity. In the frame rotating with respect to the driving frequency ω_{d}, the Hamiltonian describing this system reads ($\hbar = 1$)

$$H = H_s + H_{dr}, \tag{1}$$

where

$$H_s = \Delta_c a^\dagger a + \omega_m b^\dagger b + g a^\dagger a \left(b^\dagger + b\right)^2 \tag{2}$$

is the Hamiltonian of the quadratically coupled optomechanical system without driving term, $\Delta_c = \omega_c - \omega_{\mathrm{d}}$ is the detuning between the cavity mode and driving field, ω_m is the frequency of mechanical mode b, and g denotes the single-photon quadratic coupling strength. $H_{dr} = \Omega\left(a^\dagger + a\right)$ is the Hamiltonian representing the coupling between cavity and the driving field with laser amplitude Ω and frequency ω_{d} in the rotating picture. The evolution of this system with the relevant dissipations is then governed by the quantum Langevin equations

$$\begin{aligned}
\dot{a} &= -\left(\mathrm{i}\Delta_c + \frac{\kappa}{2}\right) a - \mathrm{i}g a \left(b^\dagger + b\right)^2 - \mathrm{i}\Omega + \sqrt{\kappa} a_{in}, \\
\dot{b} &= -\left(\mathrm{i}\omega_m + \frac{\gamma}{2}\right) b - 2\mathrm{i}g a^\dagger a \left(b^\dagger + b\right) + \sqrt{\gamma} b_{in},
\end{aligned} \tag{3}$$

where κ (γ) is the decay rate of the optical (mechanical) mode and a_{in} (b_{in}) denotes the input noise operator. Following the standard linearization procedure, the cavity and mechanical modes can be written as a sum of an average value and a quantum fluctuation term for a sufficiently strong driving field, i.e., $a \to \alpha + a$ and $b \to \beta + b$. Inserting these expressions into Eq. (3), one can derive the amplitudes $\alpha = \Omega/\left(-\Delta_c + \mathrm{i}\kappa/2\right)$ and $\beta = 0$ in the steady-state case. Then the driven-displaced Hamiltonian is given by

$$H_{dis} = \Delta_c a^\dagger a + \omega_m b^\dagger b + g\alpha \left(a^\dagger + a\right)\left(b^\dagger + b\right)^2, \tag{4}$$

when neglecting the high-order term $g a^\dagger a \left(b^\dagger + b\right)^2$. Taking the cavity coherently driven near resonance ($\Delta_c \ll \omega_m$) and $g\alpha \ll \omega_m$ into account, the rapidly oscillating terms with high frequencies $\pm 2\omega_m$ can be safely omitted under the rotating-wave approximation. Thus the Hamiltonian of the system can be approximately expressed as

$$H_{app} = \Delta_c a^\dagger a + \omega_m b^\dagger b + G\left(a^\dagger + a\right)\left(b^\dagger b + \frac{1}{2}\right), \tag{5}$$

with the enhanced coupling strength $G = 2g\alpha$. Furthermore, in order to realize phonon blockade by exploiting the anharmonicity ladder of energy spectrum in Eq. (5), a weak field with the frequency ω_p and the amplitude ε is used to drive the mechanical mode, whose corresponding Hamiltonian is described by $H_p = \varepsilon\left(b^\dagger \mathrm{e}^{-\mathrm{i}\omega_p t} + b\mathrm{e}^{\mathrm{i}\omega_p t}\right)$. The full Hamiltonian is written as

$$H'_{tot} = \Delta_c a^\dagger a + \omega_m b^\dagger b + G\left(a^\dagger + a\right)\left(b^\dagger b + \frac{1}{2}\right) + H_p. \tag{6}$$

By performing a rotating transformation with respect to $\omega_p b^\dagger b$, the Hamiltonian (6) becomes

$$\begin{aligned}
H_{tot} =& \Delta_c a^\dagger a + \Delta_m b^\dagger b + G\left(a^\dagger + a\right)\left(b^\dagger b + \frac{1}{2}\right) \\
&+ \varepsilon\left(b^\dagger + b\right),
\end{aligned} \tag{7}$$

in which $\Delta_m = \omega_m - \omega_p$ is the detuning of the mechanical mode and the weak pump field. Here we mainly consider that the phonon blockade can occur under the strong optomechanical coupling, so that the mechanical mode is confined in the two lowest-energy levels ($|0\rangle_b$, $|1\rangle_b$). Then we can approximately rewrite the creation (annihilation) operator of the mechanical mode as $b^\dagger = |1\rangle_{bb}\langle 0| = \sigma^\dagger$ ($b = |0\rangle_{bb}\langle 1| = \sigma$). In this case, the Hamiltonian in Eq.(7) takes the form

$$\begin{aligned}
H_{eff} =& \Delta_c a^\dagger a + \Delta_m \sigma^\dagger \sigma + G\left(a^\dagger + a\right)\left(\sigma^\dagger \sigma + \frac{1}{2}\right) \\
&+ \varepsilon\left(\sigma^\dagger + \sigma\right).
\end{aligned} \tag{8}$$

This approximate effective Hamiltonian will be the starting point of this work as seen in the next sections. In order to check the validity of the approximation from Hamiltonian (8) to Hamiltonian (7), we employ the quantum master equation to numerically investigate the above analytic treatment. The dynamic behavior of the total open system is described by the master equation for the density matrix ρ

$$\dot{\rho} = -\mathrm{i}\left[H, \rho\right] + \kappa\mathcal{L}\left[a\right] + \gamma\left(\bar{n}_{th} + 1\right)\mathcal{L}\left[\sigma\right] + \gamma\bar{n}_{th}\mathcal{L}\left[\sigma^\dagger\right], \tag{9}$$

where $\mathcal{L}\left[o\right] = \left(2o\rho o^\dagger - o^\dagger o\rho - \rho o^\dagger o\right)/2$ is the Lindblad super-operator for a given operator $o = b, \sigma$, and $\bar{n}_{th}$ denotes the thermal phonon number in the mechanical mode. In Fig. 2(a), we display the comparison of mean phonon number and qubit population by solving numerically master equation with Hamiltonian H_{tot} (red sphere) and Hamiltonian H_{eff} (blue solid line). We see that the two results are basically consistent. Particularly, the results agree very well with each other in single-phonon resonance cases. More specifically, the peaks in Fig. 2(a) show several resolved resonances and arise from the

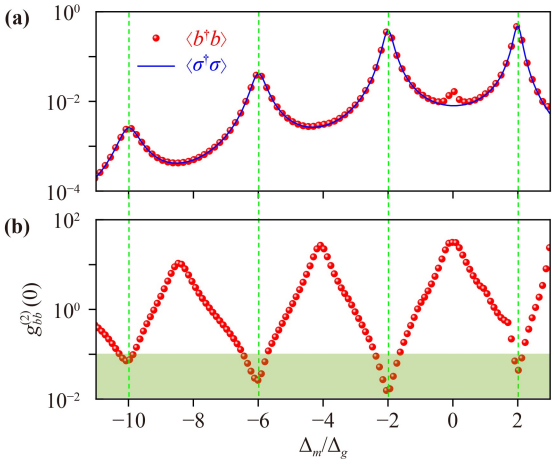

Fig. 2 **(a)** Steady-state mean phonon number $\langle b^\dagger b\rangle$ and mean atomic excited-state probability $\langle\sigma^\dagger\sigma\rangle$ governed respectively by the Hamiltonians (7) and (8) as functions of the detuning Δ_m/Δ_g. **(b)** Steady-state equal-time second-order phonon correlation function $g^{(2)}_{bb}(0)$ as a function of Δ_m/Δ_g. The other parameters are $\Delta_c/G=2$, $\Delta_g=G^2/\Delta_c$, $\kappa/G=0.1$, $\gamma=0.01\kappa$, $\varepsilon/\kappa=0.1$, and $\bar{n}_{th}=0$.

transitions between the vacuum state $|0,0\rangle$ and the manifold of single-phonon state $|\tilde{n}(1),1\rangle$ with $|\tilde{n}(1)\rangle$ being a phonon-dependent displaced number state. Accordingly, the dips in Fig. 2(b), corresponding to the single-phonon resonance transition with $\Delta_m=2G^2/\Delta_c-n\Delta_c$, indicate the occurrence of phonon blockade in the photon sidebands. In this work, we focus on the single-phonon resonances and hence only consider the case of phonon blockade, so that we can carry out our calculation with H_{eff} instead of H_{tot} for simplicity.

3 Multiple-photon generation and super-Rabi oscillation

To discuss the generation of multi-photon state and the super-Rabi oscillation between the zero-photon state and the n-photon $(n=2,3)$ state, we first apply the displacement operation

$$U_d=\exp\left[\frac{G}{\Delta_c}\left(a^\dagger-a\right)\left(\sigma^\dagger\sigma+\frac{1}{2}\right)\right] \tag{10}$$

to the first three terms $H_{th}=\Delta_c a^\dagger a+\Delta_m\sigma^\dagger\sigma+G\left(\sigma^\dagger\sigma+\frac{1}{2}\right)\left(a^\dagger+a\right)$ of Eq. (8), then this Hamiltonian becomes

$$H_{th}=\Delta_c a^\dagger a+\left(\Delta_m-\frac{2G^2}{\Delta_c}\right)\sigma^\dagger\sigma, \tag{11}$$

which satisfies

$$H_{th}\left|n,0\,(1)\right\rangle=E_{n,g(e)}\left|n,0\,(1)\right\rangle \tag{12}$$

with eigenstates $|n,0\,(1)\rangle\equiv|n\rangle_a\otimes|0\,(1)\rangle_b$ and corresponding eigenvalues

$$E_{n,0}=n\Delta_c,\ E_{n,1}=n\Delta_c+\Delta_m-\frac{2G^2}{\Delta_c}, \tag{13}$$

where $|n,0\rangle$ ($|n,1\rangle$) stands for the cavity mode being in n-photon Fock state and the mechanical mode being in zero-phonon (single-phonon) state in the displaced frame. When carrying out the inverse transformation, the eigenstate $|n,0\,(1)\rangle$ turns into the displaced state $|\tilde{n},0\,(1)\rangle=U_d\,|n,0\,(1)\rangle$ with

$$|\tilde{n}\rangle=\mathrm{e}^{\frac{G}{\Delta_c}\left(a-a^\dagger\right)\left(\sigma^\dagger\sigma+\frac{1}{2}\right)}\,|n\rangle_a \tag{14}$$

being a phonon-dependent displaced Fock state of cavity mode. Obversely, $|\tilde{n}\rangle$ has a highly adjustable displaced value through tuning the detuning Δ_c.

With the aid of completeness of $|n,0\,(1)\rangle$, H_{th} can then be put into the form

$$H_{th}=\sum_{n=0}^{\infty}\sum_{s=0,1}E_{n,s}\,|n,s\rangle\langle n,s|\,. \tag{15}$$

In the rotating frame defined by the unitary operator $\exp(-\mathrm{i}H_{th}t)$, the system Hamiltonian is expressed as

$$H_I=\varepsilon\sum_{l,n=0}^{\infty}\mathrm{e}^{\mathrm{i}(E_{n,1}-E_{l,0})t}\,{}_a\langle n|\,\mathrm{e}^{\frac{G}{\Delta_c}\left(a^\dagger-a\right)}\,|l\rangle_a\,|n,1\rangle\langle l,0|+\mathrm{H.c.}. \tag{16}$$

We choose the weak driving frequency ω_p meeting the single-phonon resonance transition of $|n,1\rangle\longleftrightarrow|0,0\rangle$ (i.e., $n\Delta_c+\Delta_m-2G^2/\Delta_c=0$). Then the fast oscillating terms can be safely eliminated under the rotating-wave approximation. Meanwhile the phonon blockade can take place in the n-photon sidebands. The Hamiltonian Eq.(16) consequently reduces

$$\begin{aligned}\tilde{H}_I=&\varepsilon\sum_{n=0}^{\infty}{}_a\langle n|\,G/\Delta_c\rangle_a\,|n,1\rangle\langle 0,0|+\mathrm{H.c.}\\=&\varepsilon\sum_{n=0}^{\infty}\Omega^{(n)}_{\mathrm{eff}}\,|n,1\rangle\langle 0,0|+\mathrm{H.c.},\end{aligned} \tag{17}$$

where $|G/\Delta_c\rangle_a$ denotes the cavity field in the coherent state and $\Omega^{(n)}_{\mathrm{eff}}=\exp\left[-G^2/\left(2\Delta_c^2\right)\right]\left(G/\Delta_c\right)^n\varepsilon/\sqrt{n!}$ is effective coupling strengths that can be conveniently controlled by choosing the detuning Δ_c. Thus the transfer from zero-photon states $|0,0\rangle$ to n photon states $|n,1\rangle$ is achieved via these effective couplings. In other words, one can obtain the multi-photon state $|n,1\rangle$ from Eq. (17) when the system is initially in the ground state $|0,0\rangle$. In Fig. 3, we plot the populations of the states $|0,0\rangle$ and $|n,1\rangle$ $(n=2,3)$ as functions of the scaled evolution time Gt, which display the essentially perfect super-Rabi oscillations in the absence of dissipation. The red and blue curves are obtained by numerically solving the Schrödinger equation with the full Hamiltonian in Eq.

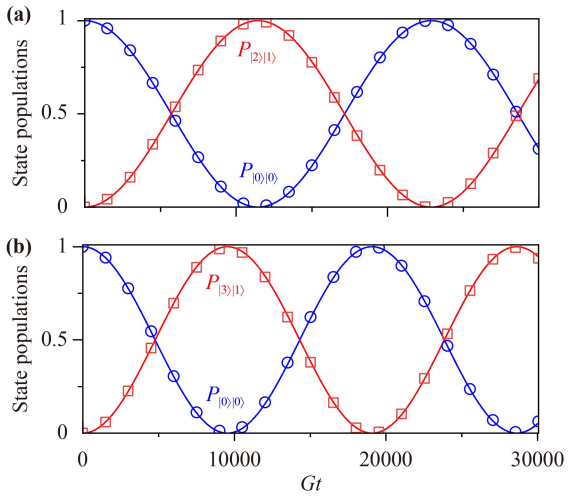

Fig. 3 The state populations $P_{|n\rangle_p|1\rangle}$ and $P_{|0\rangle_p|0\rangle}$ ($n = 2$ and 3) are plotted as functions of the scaled time Gt in **(a)** for $n = 2$, $\Delta_c/G = 7.14$, $\Delta_m = 2G^2/\Delta_c - 2\Delta_c$ and in **(b)** for $n = 3$, $\Delta_c/G = 2.86$, $\Delta_m = 2G^2/\Delta_c - 3\Delta_c$, and the common parameter $\varepsilon/G = 0.01$. The red and blue curves correspond to the numerical results of the state populations, while the red square and blue circle correspond to the analytical results based on the effective Rabi frequencies $\Omega^{(2)}_{eff}$ and $\Omega^{(3)}_{eff}$.

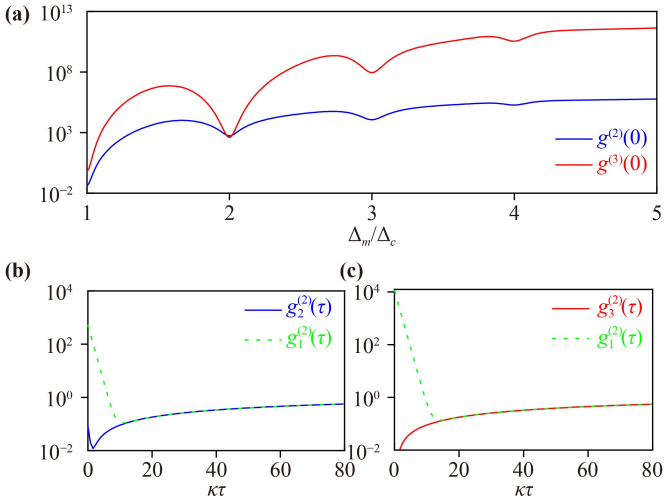

Fig. 4 **(a)** Zero-delay nth-order photon correlation functions $g^{(n)}(0)$ versus Δ_m/Δ_c. **(b, c)** The generalized time-delay second-order correlation functions $g_N^{(2)}(\tau)$ as functions of the scaled evolution time $\kappa\tau$ for $N = 2$ at (b) $\Delta_m = 2G^2/\Delta_c - 2\Delta_c$, and at (c) $\Delta_m = 2G^2/\Delta_c - 3\Delta_c$. The other parameters are $\kappa = 1$, $G/\kappa = 10$, $\Delta_c/G = 2$, $\gamma/\kappa = 0.01$, and $\varepsilon/\kappa = 0.1$, and $\bar{n}_{th} = 0$.

(8), as well as the marked ones are based on the analytical result given in Eq. (17). We clearly see from Fig. 3 that the super-Rabi oscillations emerge between the two states $|0,0\rangle$ and $|n,1\rangle$ ($n = 2,3$) for simulations and the effective analytic descriptions match the numerical results very well.

4 Multiple-photon bundle emission

The super-Rabi oscillation between the states $|0,0\rangle$ and $|n,1\rangle$ on the basis of the phonon blockade provides a physical mechanism to preparate n-photon state. However, to trigger n-photon bundle emission, the system dissipation has to be taken into account since the dissipation provides an effective radiation channel. Additionally, the condition $\kappa \gg \gamma$ must be satisfied for greatly restraining the occurrence of the harmful transition $|n,1\rangle \to |n,0\rangle$. Inasmuch as the equal-time nth-order photon correlation function defined as $g^{(n)}(0) = \langle a^{\dagger n} a^n\rangle/\langle a^\dagger a\rangle^n$can reveal strong correlation of the emitted photons, we now first employ this function to analyze the quantum statistics of the n-photon states. Concretely, we mainly consider the 2-photon and 3-photon cases in the following discussion by numerically solving the quantum master equation in Eq. (9). Figure 4(a) exhibits the equal-time n th-order correlation functions ($n = 2,3$) as functions of the scaled detuning Δ_m/Δ_c. It is clearly seen that some sharp dips instead of bunching peaks are observed for each $g^{(n)}(0)$ at n-photon resonance points $\Delta_m = 2G^2/\Delta_c - n\Delta_c$, which manifests that the cavity emits its energy in the manner of antibunched n-photon bundles. To further characterize the bunching or antibunching effect between the n-photon bundles, we calculate the generalized time-delay second-order correlation function of N-photon bundle

$$g_N^{(2)}(\tau) = \frac{\langle a^{\dagger N}(0)\, a^{\dagger N}(\tau)\, a^N(\tau)\, a^N(0)\rangle}{\langle (a^{\dagger N} a^N)(0)\rangle \langle (a^{\dagger N} a^N)(\tau)\rangle}, \tag{18}$$

where the N-photon emission events are considered as a basic unit and $g_1^{(2)}(\tau)$ is exactly the standard time-delay second-order correlation function for the case of $N = 1$. The numerical result in Fig. 4(b) depicts that $g_1^{(2)}(0) > g_1^{(2)}(\tau)$ and $g_2^{(2)}(0) < g_2^{(2)}(\tau)$ are simultaneously satisfied in the case of $\Delta_m = 2G^2/\Delta_c - 2\Delta_c$, which implies that the photons contained in each 2-photon pair take on bunching behavior and yet the relation between adjacent 2-photon pairs are antibunched. Similarly, we observe $g_1^{(2)}(0) > g_1^{(2)}(\tau)$ and $g_3^{(2)}(0) < g_3^{(2)}(\tau)$ for $\Delta_m = 2G^2/\Delta_c - 3\Delta_c$ in Fig. 4(c), hence the strongly correlated 3-photon bundles can also be generated. Considering that the order n of the bundle can be controlled simply by adjusting the frequency of the pumping laser, our proposal realizes a versatile optically controlled multi-photon source.

To exhibit the multi-photon bundle emission process more clearly, we now apply the quantum Monte Carlo simulation to track the individual quantum trajectories of the system. The emission event is recorded whenever the system undergoes a quantum jump. Figures 5(a–c) present a small fraction of a quantum trajectory of the state populations $P_{|m\rangle|0(1)\rangle}$ ($m = 0,1,2$) when $n = 2$ and

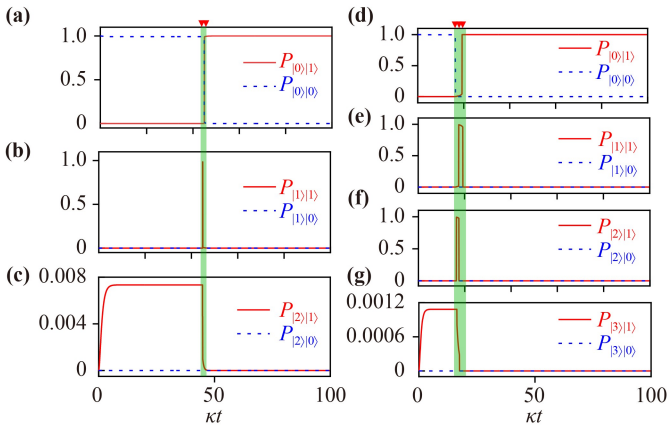

Fig. 5 Small fraction of one quantum trajectory of the state populations $P_{|n\rangle|0(1)\rangle}$ $(n = 0, 1, 2, 3)$ at **(a–c)** $G/\kappa = 10$ and $\Delta_m = 2G^2/\Delta_c - 2\Delta_c$, corresponding to the two-photon bundle emission; **(d–g)** $G/\kappa = 30$ and $\Delta_m = 2G^2/\Delta_c - 3\Delta_c$, corresponding to the three-photon bundle emission. The other parameters are $\Delta_c = G$, $\gamma/\kappa = 0.01$, $\varepsilon/\kappa = 0.2$, and $\bar{n}_{th} = 0$.

$\Delta_m = 2G^2/\Delta_c - 2\Delta_c$. Here we consider the system is initially in the state $|0\rangle|0\rangle$. At first, the super-Rabi oscillation causes that two-photon state $|2, 1\rangle$ is occupied with a probability close to 0.8%. As time goes on, the system emits one photon denoted by the first red triangle and then the wave function collapses into the state $|1, 1\rangle$ with almost unit probability. Immediately, the second photon is emitted within the cavity lifetime (the second red triangle). Thus a bundle of two photons is emitted in a very short temporal window. The system then remains in the state $|0, 1\rangle$ for a long time until two photon state is constructed again after a phonon emission. In Figs. 5(d–g), we show a short duration of a quantum trajectory of the state populations $P_{|m\rangle|0(1)\rangle}$ $(m = 0, 1, 2, 3)$ when $n = 3$ and $\Delta_m = 2G^2/\Delta_c - 3\Delta_c$. It can be seen that the 3-photon bundle emission can be realized in the same fashion way.

5 Discussion and conclusion

In this section we first discuss the experimental prospect of our proposal. To implement the present scheme, the key challenge is to realize the ultrastrong optomechanical coupling condition (i.e., $G > \kappa$). Currently, the single-photon quadratic coupling strength g has been enhanced to 245 Hz in the photonic crystal optomechanical cavity [68], and likely enhanced to 100 kHz by carefully tuning the double-slotted photonic crystal structure, and then the effective coupling strength $G = 2g\alpha$ can attain hundreds of MHz for $\alpha \sim 10^4$ through adjusting the amplitude of driving field [69]. Therefore, the condition $G > \kappa$ is possibly implemented in the photonic crystal cavity with the current experimental technology [70]. Besides that, an effective alternative approach to generating ultrastrong optomechanical coupling is to periodically modulate the membrane [71]. In this situation, the modulation of the spring constant gives rise to a mechanical parametric amplification with frequency $2\omega_d'$, amplitude χ, and phase φ. Then in a frame rotating of frequency ω_d', the Hamiltonian of the mechanical oscillation reads

$$H_m = \Delta_m b^\dagger b + \frac{\chi}{2}\left(b^{\dagger 2}\mathrm{e}^{-\mathrm{i}\varphi} + b^2\mathrm{e}^{\mathrm{i}\varphi}\right), \tag{19}$$

in which the detuned mechanical parametric oscillator is stable in the region of $\chi < \Delta_m = \omega_m - \omega_d'$. The quadratical coupling between the cavity and mechanical modes in the rotating frame of the modulation frequency is given by

$$H_{om} = ga^\dagger a\left(b^\dagger \mathrm{e}^{\mathrm{i}\omega_d' t/2} + b\mathrm{e}^{-\mathrm{i}\omega_d' t/2}\right)^2. \tag{20}$$

Under the condition of $\omega_d' \gg g$ and ignoring the shift of cavity frequency caused by the term $ga^\dagger a$, the interaction can be usually simplified as $H_{om} = 2ga^\dagger a b^\dagger b$ by employing the rotating-wave approximation. When introducing a squeezed mechanical mode b_v via Bogoliubov transformation $b_v = b\cosh r_d + b^\dagger \mathrm{e}^{-\mathrm{i}\varphi}\sinh r_d$ with $r_d = \frac{1}{4}\ln\frac{\Delta+\chi}{\Delta-\chi}$ and $\Delta_v = \frac{\Delta}{\cosh 2r_d}$, we have $H_m = \Delta_v b_v^\dagger b_v$ and

$$\begin{aligned} H_{om} =& 2ga^\dagger a\left(b_v^\dagger\cosh r_d - b_v\mathrm{e}^{\mathrm{i}\varphi}\sinh r_d\right) \\ &\times\left(b_v\cosh r_d - b_v^\dagger\mathrm{e}^{-\mathrm{i}\varphi}\sinh r_d\right). \end{aligned} \tag{21}$$

Assuming that $\varphi = \pi$ and a large amplification $(\mathrm{e}^{2r_d} \gg 1)$, we easily find

$$H_{om} = \frac{1}{2}g\mathrm{e}^{2r_d}a^\dagger a\left(b_v^\dagger + b_v\right)^2. \tag{22}$$

Eq. (22) indicates that an exponentially enhanced single-photon coupling strength $g\mathrm{e}^{2r_d}/2$ can be obtained. However, it is noticed that the mechanical paramtetric process will unavoidably increase the influence of mechanical noise. According to Ref. [71], here we point out that this amplified noise can be suppressed by introducing a broadband squeezed vacuum reservoir of the mechanical mode b_v with a phase matching condition. In addition, the cavity is driven by a strong laser field in our model, which means that the emission of photon bundles is accompanied by a classical coherent field. In order to distinguish the two emitted signals and only observe that of emitted photon bundles, an ancillary cavity of operator c and frequency ω_c is used to couple the optomechanical cavity and driven by a weak probe field [72]. Its dynamics is described by

$$\dot{c} = -\left(\mathrm{i}\Delta_c + \kappa_c\right)c - \mathrm{i}g_{ac}a + \sqrt{2\kappa_c}c_{in}, \tag{23}$$

where κ_c, Δ_c, g_{ac} and c_{in} are the relevant damping rate, effective detuning, coupling strength, and input noise, respectively. Using the input-output relation $c_{out} = \sqrt{2\kappa_c}c - c_{in}$, we finally get

$$c_{out} = -\mathrm{i}\sqrt{2}g_{ac}/\sqrt{\kappa_c}a + c_{in}, \quad (24)$$

which brings about a state swap between two cavity modes, and then the signal of emitted photon bundles can be monitored by directly measuring the ancillary cavity output c_{out}.

In summary, we have studied the dynamical emission of multiple-photon states based on the phonon blockade in the optomechanical system with quadratic coupling. Through characterizing the mechanical mode only with its two lowest-energy levels when the phonon blockade happens in the photon sidebands and carrying out the displaced transformation, we obtain the super-Rabi oscillations between the vacuum state $|0,0\rangle$ and the n-photon states with one phonon $|n,1\rangle$, in which the effective super-Rabi frequencies can be conveniently controlled by tuning the detuning between the cavity mode and driving field. The n-photon bundle emission has been revealed by numerically calculating several typical correlation functions and the quantum Monter Carlo simulations. Especially, we have demonstrated that the release of single-phonon can act as a signal to predict the cascade emission of antibunched n-photon bundles. Hence our scheme simultaneously realizes antibunched multiple-photon emitter and single-phonon gun in the optomechanical system. We expect that this nonclassical source may have valuable applications in quantum information processing.

Declarations The authors declare that they have no competing interests and there are no conflicts.

Data availability Data underlying the results presented in this paper are not publicly available at this time but may be obtained from the authors upon reasonable request.

Acknowledgements Y.-J. Xu is supported by the National Science Foundation for Distinguished Young Scholars of the Higher Education Institutions of Anhui Province under Grant No. 2022AH020097, the Excellent Scientific Research and Innovation Team of Anhui Colleges under Grant No. 2022AH010098, and the Collaborative Innovation Project of University of Anhui Province under Grant No. GXXT-2022-088. H. Xie is supported by the National Natural Science Foundation of China under Grant No. 12174054.

References

1. V. Giovannetti, S. Lloyd, and L. Maccone, Quantum metrology, *Phys. Rev. Lett.* 96(1), 010401 (2006)
2. L. Pezzè, A. Smerzi, M. K. Oberthaler, R. Schmied, and P. Treutlein, Quantum metrology with nonclassical states of atomic ensembles, *Rev. Mod. Phys.* 90(3), 035005 (2018)
3. D. Braun, G. Adesso, F. Benatti, R. Floreanini, U. Marzolino, M. W. Mitchell, and S. Pirandola, Quantum-enhanced measurements without entanglement, *Rev. Mod. Phys.* 90(3), 035006 (2018)
4. L. M. Duan, M. D. Lukin, J. I. Cirac, and P. Zoller, Long-distance quantum communication with atomic ensembles and linear optics, *Nature* 414(6862), 413 (2001)
5. P. Kok, W. J. Munro, K. Nemoto, T. C. Ralph, J. P. Dowling, and G. J. Milburn, Linear optical quantum computing with photonic qubits, *Rev. Mod. Phys.* 79(1), 135 (2007)
6. H. J. Kimble, The quantum internet, *Nature* 453(7198), 1023 (2008)
7. I. Afek, O. Ambar, and Y. Silberberg, High-NOON states by mixing quantum and classical light, *Science* 328(5980), 879 (2010)
8. M. D'Angelo, M. V. Chekhova, and Y. Shih, Two-photon diffraction and quantum lithography, *Phys. Rev. Lett.* 87(1), 013602 (2001)
9. K. E. Dorfman, F. Schlawin, and S. Mukamel, Nonlinear optical signals and spectroscopy with quantum light, *Rev. Mod. Phys.* 88(4), 045008 (2016)
10. J. C. López Carreño, C. Sánchez Muñoz, D. Sanvitto, E. del Valle, and F. P. Laussy, Exciting polaritons with quantum light, *Phys. Rev. Lett.* 115(19), 196402 (2015)
11. Z. R. Zhong, X. Wang, and W. Qin, Towards quantum entanglement of micromirrors via a two-level atom and radiation pressure, *Front. Phys.* 13(5), 130319 (2018)
12. J. H. Liu, Y. B. Zhang, Y. F. Yu, and Z. M. Zhang, Photon–phonon squeezing and entanglement in a cavity optomechanical system with a flying atom, *Front. Phys.* 14(1), 12601 (2019)
13. C. S. Muñoz, E. del Valle, A. G. Tudela, K. Müller, S. Lichtmannecker, M. Kaniber, C. Tejedor, J. J. Finley, and F. P. Laussy, Emitters of *N*-photon bundles, *Nat. Photonics* 8(7), 550 (2014)
14. C. Sánchez Muñoz, F. P. Laussy, E. Valle, C. Tejedor, and A. González-Tudela, Filtering multiphoton emission from state-of-the-art cavity quantum electrodynamics, *Optica* 5(1), 14 (2018)
15. Q. Bin, X. Y. Lü, F. P. Laussy, F. Nori, and Y. Wu, *N*-phonon bundle emission via the Stokes process, *Phys. Rev. Lett.* 124(5), 053601 (2020)
16. Q. Bin, Y. Wu, and X. Y. Lü, Parity–symmetry-protected multiphoton bundle emission, *Phys. Rev. Lett.* 127(7), 073602 (2021)
17. Y. Deng, T. Shi, and S. Yi, Motional *n*-phonon bundle states of a trapped atom with clock transitions, *Photon. Res.* 9(7), 1289 (2021)
18. S. Y. Jiang, F. Zou, Y. Wang, J. F. Huang, X. W. Xu, and J. Q. Liao, Multiple-photon bundle emission in the *n*-photon Jaynes–Cummings model, *Opt. Express* 31(10), 15697 (2023)
19. C. Liu, J. F. Huang, and L. Tian, Deterministic generation of multi-photon bundles in a quantum Rabi model, *Sci. China Phys. Mech. Astron.* 66(2), 220311 (2023)
20. A. González-Tudela, V. Paulisch, D. E. Chang, H. J. Kimble, and J. I. Cirac, Deterministic generation of arbitrary photonic states assisted by dissipation, *Phys. Rev. Lett.* 115(16), 163603 (2015)
21. J. S. Douglas, T. Caneva, and D. E. Chang, Photon molecules in atomic gases trapped near photonic crystal waveguides, *Phys. Rev. X* 6(3), 031017 (2016)
22. A. González-Tudela, V. Paulisch, H. J. Kimble, and J. I.

Cirac, Efficient multiphoton generation in waveguide quantum electrodynamics, *Phys. Rev. Lett.* 118(21), 213601 (2017)
23. S. L. Ma, X. K. Li, Y. L. Ren, J. K. Xie, and F. L. Li, Antibunched *N*-photon bundles emitted by a Josephson photonic device, *Phys. Rev. Res.* 3(4), 043020 (2021)
24. Y. Ota, S. Iwamoto, N. Kumagai, and Y. Arakawa, Spontaneous two-photon emission from a single quantum dot, *Phys. Rev. Lett.* 107(23), 233602 (2011)
25. G. Callsen, A. Carmele, G. Hönig, C. Kindel, J. Brunnmeier, M. R. Wagner, E. Stock, J. S. Reparaz, A. Schliwa, S. Reitzenstein, A. Knorr, A. Hoffmann, S. Kako, and Y. Arakawa, Steering photon statistics in single quantum dots: From one- to two-photon emission, *Phys. Rev. B* 87(24), 245314 (2013)
26. C. Sánchez Muñoz, F. P. Laussy, C. Tejedor, and E. Valle, Enhanced two-photon emission from a dressed biexciton, *New J. Phys.* 17(12), 123021 (2015)
27. Y. Chang, A. González-Tudela, C. Sánchez Muñoz, C. Navarrete-Benlloch, and T. Shi, Deterministic down-converter and continuous photon-pair source within the bad-cavity limit, *Phys. Rev. Lett.* 117(20), 203602 (2016)
28. X. L. Dong and P. B. Li, Multiphonon interactions between nitrogen–vacancy centers and nanomechanical resonators, *Phys. Rev. A* 100(4), 043825 (2019)
29. P. Bienias, S. Choi, O. Firstenberg, M. F. Maghrebi, M. Gullans, M. D. Lukin, A. V. Gorshkov, and H. P. Büchler, Scattering resonances and bound states for strongly interacting Rydberg polaritons, *Phys. Rev. A* 90(5), 053804 (2014)
30. M. F. Maghrebi, M. J. Gullans, P. Bienias, S. Choi, I. Martin, O. Firstenberg, M. D. Lukin, H. P. Büchler, and A. V. Gorshkov, Coulomb bound states of strongly interacting photons, *Phys. Rev. Lett.* 115(12), 123601 (2015)
31. F. Zou, J. Q. Liao, and Y. Li, Dynamical emission of phonon pairs in optomechanical systems, *Phys. Rev. A* 105(5), 053507 (2022)
32. H. Y. Yuan, J. K. Xie, and R. A. Duine, Magnon bundle in a strongly dissipative magnet, *Phys. Rev. Appl.* 19(6), 064070 (2023)
33. M. Aspelmeyer, T. J. Kippenberg, and F. Marquardt, Cavity optomechanics, *Rev. Mod. Phys.* 86(4), 1391 (2014)
34. T. J. Kippenberg and K. J. Vahala, Cavity optomechanics: Back-action at the mesoscale, *Science* 321(5893), 1172 (2008)
35. M. Aspelmeyer, P. Meystre, and K. Schwab, Quantum optomechanics, *Phys. Today* 65(7), 29 (2012)
36. P. Meystre, A short walk through quantum optomechanics, *Ann. Phys.* 525(3), 215 (2013)
37. H. Xiong, L. G. Si, X. Y. Lü, X. X. Yang, and Y. Wu, Review of cavity optomechanics in the weak-coupling regime: From linearization to intrinsic nonlinear interactions, *Sci. China Phys. Mech. Astron.* 58(5), 1 (2015)
38. A. Nunnenkamp, K. Børkje, and S. M. Girvin, Single-photon optomechanics, *Phys. Rev. Lett.* 107(6), 063602 (2011)
39. J. Q. Liao, H. K. Cheung, and C. K. Law, Spectrum of single-photon emission and scattering in cavity optomechanics, *Phys. Rev. A* 85(2), 025803 (2012)
40. P. Kómár, S. D. Bennett, K. Stannigel, S. J. M. Habraken, P. Rabl, P. Zoller, and M. D. Lukin, Single-photon nonlinearities in two-mode optomechanics, *Phys. Rev. A* 87(1), 013839 (2013)
41. T. Hong, H. Yang, H. Miao, and Y. Chen, Open quantum dynamics of single-photon optomechanical devices, *Phys. Rev. A* 88(2), 023812 (2013)
42. J. Q. Liao and F. Nori, Single-photon quadratic optomechanics, *Sci. Rep.* 4(1), 6302 (2014)
43. J. Q. Liao and L. Tian, Macroscopic quantum superposition in cavity optomechanics, *Phys. Rev. Lett.* 116(16), 163602 (2016)
44. H. Xie, G. W. Lin, X. Chen, Z. H. Chen, and X. M. Lin, Single-photon nonlinearities in a strongly driven optomechanical system with quadratic coupling, *Phys. Rev. A* 93(6), 063860 (2016)
45. X. W. Xu, A. X. Chen, and Y. X. Liu, Phonon blockade in a nanomechanical resonator resonantly coupled to a qubit, *Phys. Rev. A* 94(6), 063853 (2016)
46. H. Xie, C. G. Liao, X. Shang, M. Y. Ye, and X. M. Lin, Phonon blockade in a quadratically coupled optomechanical system, *Phys. Rev. A* 96(1), 013861 (2017)
47. H. Q. Shi, X. T. Zhou, X. W. Xu, and N. H. Liu, Tunable phonon blockade in quadratically coupled optomechanical systems, *Sci. Rep.* 8(1), 2212 (2018)
48. L. L. Zheng, T. S. Yin, Q. Bin, X. Y. Lü, and Y. Wu, Single-photon-induced phonon blockade in a hybrid spin-optomechanical system, *Phys. Rev. A* 99(1), 013804 (2019)
49. T. S. Yin, Q. Bin, G. L. Zhu, G. R. Jin, and A. X. Chen, Phonon blockade in a hybrid system via the second-order magnetic gradient, *Phys. Rev. A* 100(6), 063840 (2019)
50. J. Y. Yang, Z. Jin, J. S. Liu, H. F. Wang, and A. D. Zhu, Unconventional phonon blockade in a Tavis–Cummings coupled optomechanical system, *Ann. Phys.* 532(12), 2000299 (2020)
51. P. Rabl, Photon blockade effect in optomechanical systems, *Phys. Rev. Lett.* 107(6), 063601 (2011)
52. J. Q. Liao and F. Nori, Photon blockade in quadratically coupled optomechanical systems, *Phys. Rev. A* 88(2), 023853 (2013)
53. H. Z. Shen, Y. H. Zhou, and X. X. Yi, Tunable photon blockade in coupled semiconductor cavities, *Phys. Rev. A* 91(6), 063808 (2015)
54. H. Flayac and V. Savona, Unconventional photon blockade, *Phys. Rev. A* 96(5), 053810 (2017)
55. R. Huang, A. Miranowicz, J. Q. Liao, F. Nori, and H. Jing, Nonreciprocal photon blockade, *Phys. Rev. Lett.* 121(15), 153601 (2018)
56. H. J. Snijders, J. A. Frey, J. Norman, H. Flayac, V. Savona, A. C. Gossard, J. E. Bowers, M. P. van Exter, D. Bouwmeester, and W. Löffler, Observation of the unconventional photon blockade, *Phys. Rev. Lett.* 121(4), 043601 (2018)
57. B. Sarma and A. K. Sarma, Unconventional photon blockade in three-mode optomechanics, *Phys. Rev. A* 98(1), 013826 (2018)
58. B. J. Li, R. Huang, X. W. Xu, A. Miranowicz, and H. Jing, Nonreciprocal unconventional photon blockade in

a spinning optomechanical system, *Photon. Res.* 7(6), 630 (2019)
59. D. Y. Wang, C. H. Bai, S. Liu, S. Zhang, and H. F. Wang, Distinguishing photon blockade in a PT-symmetric optomechanical system, *Phys. Rev. A* 99(4), 043818 (2019)
60. D. Y. Wang, C. H. Bai, S. Liu, S. Zhang, and H. F. Wang, Photon blockade in a double-cavity optomechanical system with nonreciprocal coupling, *New J. Phys.* 22(9), 093006 (2020)
61. Y. P. Gao, C. Cao, P. F. Lu, and C. Wang, Phase-controlled photon blockade in optomechanical systems, *Fundamental Research* 3(1), 30 (2023)
62. L. J. Feng, L. Yan, and S. Q. Gong, Unconventional photon blockade induced by the self-Kerr and cross-Kerr nonlinearities, *Front. Phys.* 18(1), 12304 (2023)
63. Z. X. Liu, H. Xiong, and Y. Wu, Magnon blockade in a hybrid ferromagnet–superconductor quantum system, *Phys. Rev. B* 100(13), 134421 (2019)
64. J. K. Xie, S. L. Ma, and F. L. Li, Quantum-interference-enhanced magnon blockade in an yttrium-iron-garnet sphere coupled to superconducting circuits, *Phys. Rev. A* 101(4), 042331 (2020)
65. Y. J. Xu, T. L. Yang, L. Lin, and J. Song, Conventional and unconventional magnon blockades in a qubit-magnon hybrid quantum system, *J. Opt. Soc. Am. B* 38(3), 876 (2021)
66. X. Y. Li, X. Wang, Z. Wu, W. X. Yang, and A. X. Chen, Tunable magnon antibunching in a hybrid ferromagnet–superconductor system with two qubits, *Phys. Rev. B* 104(22), 224434 (2021)
67. Y. M. Wang, W. Xiong, Z. Y. Xu, G. Q. Zhang, and J. Q. You, Dissipation-induced nonreciprocal magnon blockade in a magnon-based hybrid system, *Sci. China Phys. Mech. Astron.* 65(6), 260314 (2022)
68. T. K. Paraïso, M. Kalaee, L. Zang, H. Pfeifer, F. Marquardt, and O. Painter, Position-squared coupling in a tunable photonic crystal optomechanical cavity, *Phys. Rev. X* 5(4), 041024 (2015)
69. J. C. Sankey, C. Yang, B. M. Zwickl, A. M. Jayich, and J. G. Harris, Strong and tunable nonlinear optomechanical coupling in a low-loss system, *Nat. Phys.* 6(9), 707 (2010)
70. H. Sekoguchi, Y. Takahashi, T. Asano, and S. Noda, Photonic crystal nanocavity with a Q-factor of ~9 million, *Opt. Express* 22(1), 916 (2014)
71. T. S. Yin, X. Y. Lü, L. L. Zheng, M. Wang, S. Li, and Y. Wu, Nonlinear effects in modulated quantum optomechanics, *Phys. Rev. A* 95(5), 053861 (2017)
72. D. Vitali, S. Gigan, A. Ferreira, H. R. Böhm, P. Tombesi, A. Guerreiro, V. Vedral, A. Zeilinger, and M. Aspelmeyer, Optomechanical entanglement between a movable mirror and a cavity field, *Phys. Rev. Lett.* 98(3), 030405 (2007)